

Strain effects and atomic arrangements of 60° and 90° dislocations near the ZnTe/GaAs heterointerface

T. W. Kim, D. U. Lee, H. S. Lee, J. Y. Lee, and H. L. Park

Citation: *Appl. Phys. Lett.* **78**, 1409 (2001); doi: 10.1063/1.1349866

View online: <http://dx.doi.org/10.1063/1.1349866>

View Table of Contents: <http://apl.aip.org/resource/1/APPLAB/v78/i10>

Published by the [American Institute of Physics](http://www.aip.org).

Additional information on *Appl. Phys. Lett.*

Journal Homepage: <http://apl.aip.org/>

Journal Information: http://apl.aip.org/about/about_the_journal

Top downloads: http://apl.aip.org/features/most_downloaded

Information for Authors: <http://apl.aip.org/authors>

ADVERTISEMENT



Goodfellow
metals • ceramics • polymers • composites
70,000 products
450 different materials
small quantities fast

www.goodfellowusa.com

Strain effects and atomic arrangements of 60° and 90° dislocations near the ZnTe/GaAs heterointerface

T. W. Kim and D. U. Lee

Department of Physics, Kwangwoon University, 447-1 Wolgye-dong, Nowon-ku, Seoul 139-701, Korea

H. S. Lee and J. Y. Lee

Department of Materials Science and Engineering, Korea Advanced Institute of Science and Technology, 373-1 Gusung-dong, Yuseong-ku, Daejeon 305-701, Korea

H. L. Park

Department of Physics, Yonsei University, Seoul 120-749, Korea

(Received 13 March 2000; accepted for publication 18 December 2000)

Auger electron spectroscopy (AES) and secondary ion mass spectroscopy (SIMS) measurements were carried out to characterize the composition of ZnTe films, and transmission electron microscopy (TEM) measurements were performed to investigate the lattice mismatch and the microstructural properties of the ZnTe/GaAs heterostructures. The AES and SIMS results showed that the ZnTe/GaAs heterointerfaces had relatively sharp interfaces. The TEM images and the selected-area electron-diffraction patterns showed a large lattice mismatch between the ZnTe epitaxial layer and the GaAs substrate, 60° and 90° dislocations together with stacking faults, near the ZnTe/GaAs heterointerface. The ZnTe epitaxial film grown on the GaAs substrate receives a compressive strain of -0.61% , and possible atomic arrangements of the 60° and the 90° dislocations are presented on the basis of the high-resolution TEM results. © 2001 American Institute of Physics. [DOI: 10.1063/1.1349866]

The heteroepitaxial growth of II–VI/III–V strained heterostructures has attracted much attention from both scientific and technological points of view.^{1–6} However, since there are inherent problems due to possible cross-doping effects due to interdiffusion in the interfacial region^{7–9} or to strain effects as a consequence of the lattice mismatch between the II–VI quantum structures and the III–V substrates,¹⁰ relatively few studies have been devoted to the growth and the physical properties of II–VI/III–V mixed structures. Among the many kinds of II–VI/III–V heterostructures, the growth of ZnTe epilayers on various substrates has driven an extensive and successful effort due to their potential applications in the areas of optoelectronics and communications.^{11–15} However, since ZnTe/GaAs heterostructures have inherent problems due to the large lattice mismatch ($\Delta a/a = 7.6\%$ at 25 °C), studies of the microstructural properties near the ZnTe/GaAs heterostructures are very important for achieving high-quality optoelectronic devices.

This letter presents the atomic arrangements of ZnTe thin films grown on GaAs substrates by using a temperature-gradient vapor-transport deposition (TGVTD) method. Auger electron spectroscopy (AES) and secondary ion mass spectroscopy (SIMS) measurements were carried out in order to characterize the composition of the grown films. Transmission electron microscopy (TEM) and selected-area electron-diffraction measurements were performed to investigate the microstructural properties of the ZnTe/GaAs heterointerfaces. Possible atomic arrangements of the 60° and the 90° dislocations near the ZnTe/GaAs heterointerfaces are presented on the basis of the high-resolution TEM results.

The results of the AES measurements showed that the

film consisted of zinc, tellurium, and carbon at the surface of the ZnTe and of zinc and tellurium at a 1500 Å depth, as shown in Fig. 1. The existence of the carbon impurities could be due to contamination from air pollution of the ZnTe surface between growth and AES measurements. Figure 1 shows that the interfaces between the ZnTe and the GaAs were relatively abrupt and that the ZnTe film had a uniform composition throughout the layer. The thickness of ZnTe was approximately 1 μm, and that value was in good agreement with the one determined from ellipsometry. The SIMS measurements employed a very low primary ion density of around 1 nA cm⁻² and a low primary ion energy of 1 keV, and the bombarding area was approximately 10 mm². The SIMS profile of the ZnTe/GaAs heterostructure showed that the ZnTe/GaAs heterointerface was relatively sharp, as shown in Fig. 2, which was confirmed by the AES profile.

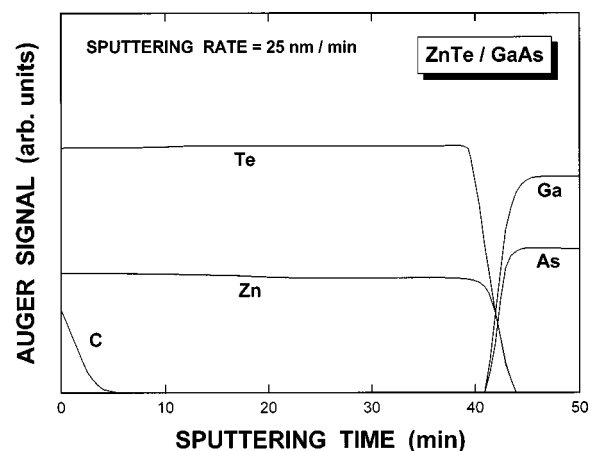


FIG. 1. Auger depth profile of the ZnTe/GaAs heterostructure.

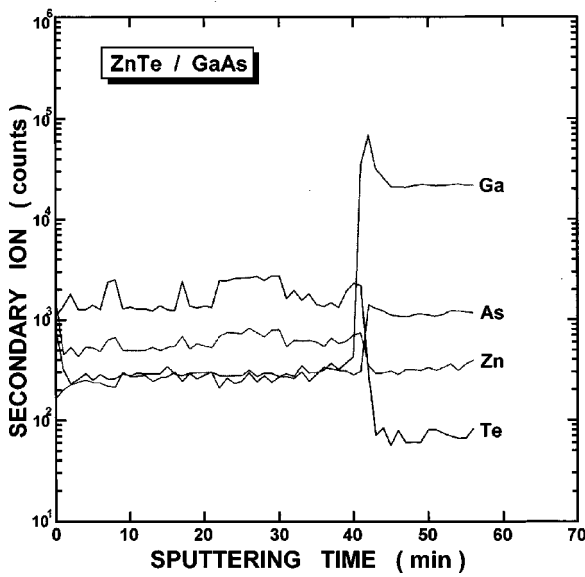


FIG. 2. Secondary ion mass spectroscopy profile of the ZnTe/GaAs heterostructure.

A selected-area electron-diffraction pattern from the ZnTe/GaAs heterointerface region is shown in Fig. 3. The electron-diffraction spots occur in pairs due to the large lattice mismatch between the ZnTe film and the GaAs substrate, with the inside spots and the smaller outside spots corresponding to the ZnTe and the GaAs, respectively. The diffraction pattern indicates that an epitaxial orientation relationship between the ZnTe and the GaAs was formed and that the ZnTe/GaAs structure was a lattice-mismatched heterostructure.

A high-resolution TEM image of a cross-sectional sample of the ZnTe/GaAs heterostructure is presented in Fig. 4. Figure 4 directly shows the lattice structures on both sides of the heteroepitaxial interface, as well as 60° and 90° dislocations, together with stacking faults, near the ZnTe/GaAs heterostructure. The number of 60° dislocations is more than the number of 90° dislocations, both of which originate from the lattice mismatch between the ZnTe epitaxial layer and the GaAs substrate. Since the activation energy of a 60° dislocation inserted into a {111} plane is lower than that of a 90°

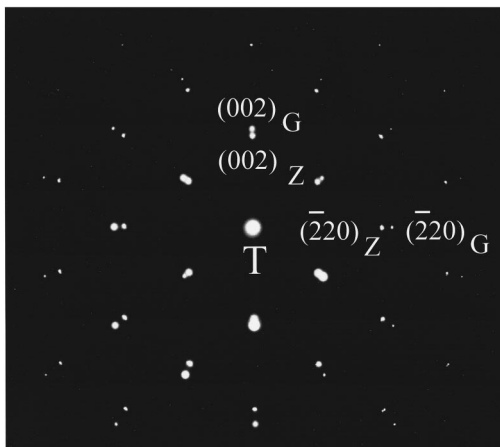


FIG. 3. An electron-diffraction pattern from transmission electron microscopy of the ZnTe/GaAs heterostructure; $(hkl)_Z$ and $(hkl)_G$ correspond to the ZnTe and the GaAs indices, respectively.

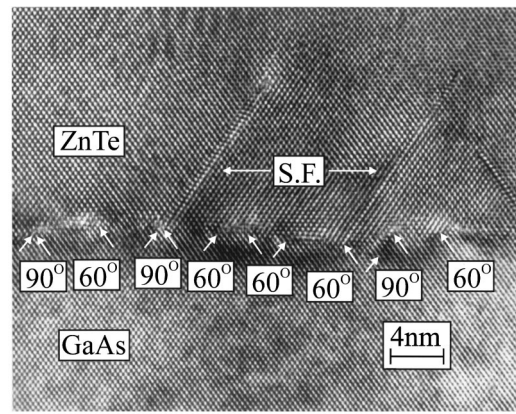


FIG. 4. A high-resolution transmission electron microscopy image of a ZnTe/GaAs heterostructure.

dislocation inserted in two {111} planes, the 60° dislocation is created easily in comparison with the 90° dislocation.^{16,17} However, since the magnitude of the strain release of the 60° dislocation is almost half that of the 90° dislocation due to the existence of the perpendicular component of the Burgers vector for the {001} interface, the 90° misfit dislocations are more efficient in relaxing the strain than the 60° dislocations. The calculated number of 90° dislocations, taking into account the strain-release effect, was approximately one per 58.3 Å.

When a ZnTe epilayer is grown on a GaAs substrate, the magnitude of the relaxation of the ZnTe epilayer can be estimated from the number of dislocations.¹⁸ The lattice mismatch (f) between the ZnTe layer and the GaAs substrate at a growth temperature of 320 °C is -7.48%, and the value of the biaxial compressive strain ($\epsilon_{||}$) is equal to f .¹⁹ When misfit dislocations are created, the elastic strain decreases, and the elastic strain relaxation (δ) existing in the ZnTe film grown on the GaAs substrate is 6.87%.²⁰ Since the actual

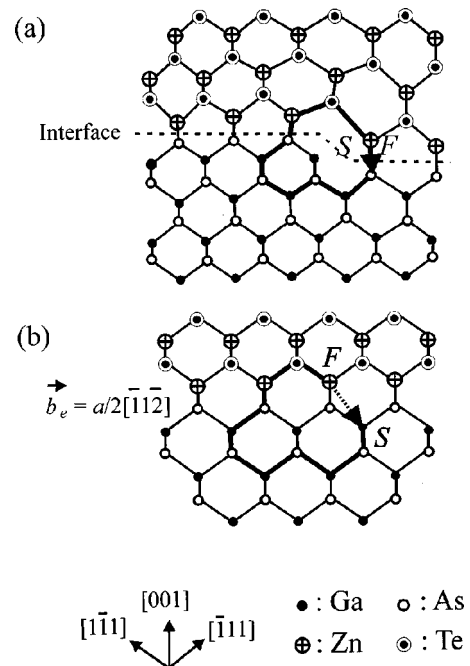


FIG. 5. Atomic arrangements of the 60° dislocation near the ZnTe/GaAs heterointerface for (a) a real crystal and (b) an ideal crystal.

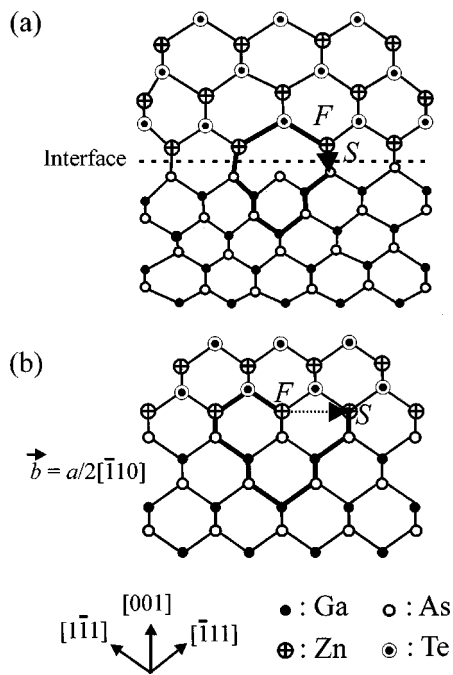


FIG. 6. Atomic arrangements of the 90° dislocation near the ZnTe/GaAs heterointerface for (a) a real crystal and (b) an ideal crystal.

total strain (ϵ_t) is equal to the sum of ϵ_{\parallel} and δ , the value of the ϵ_t existing in the ZnTe epilayer is -0.61% . The negative sign indicates that the ZnTe film receives a compressive strain. Since the value of ϵ_t totally vanishes, when the ZnTe epilayer grown on the GaAs substrate is fully relaxed, the value of δ becomes $-\epsilon_{\parallel}$. Since the spacing between misfit dislocations is defined by $-b_{\text{eff}}/f$,¹⁸ when the effective component of the Burgers vector of the dislocation ($-b_{\text{eff}}$) releases the strain, the theoretical average distance between misfit dislocations for a fully relaxed strain is about 54 \AA . The average distance between misfit dislocations, determined from high-resolution TEM images, was approximately 58.3 \AA , which was slightly larger than the theoretical value. The small difference between the experimental and the theoretical values originates from the existence of a compressive strain in the ZnTe epilayer.

The projections of the atomic arrangements of the 60° and the 90° dislocations are presented in Figs. 5 and 6 on the basis of high-resolution TEM results. Since the sense vector points into the page, the directions of all the Burgers circuits are clockwise, according to the right-hand and the finish-start conventions, as shown in Figs. 5 and 6.^{21–23} In the projection plane of the atomic arrangement of the 60° dislocations, an extra half plane and a Burgers vector exist in different planes, as shown in Fig. 5. The extra half plane is located at a $(1\bar{1}1)$ plane, and the Burgers vector (\mathbf{b}), which is $a/2[01\bar{1}]$ or $a/2[\bar{1}0\bar{1}]$, lies in a $(\bar{1}11)$ plane. The projected-edge (\mathbf{b}_e) and the screw (\mathbf{b}_s) components corresponding to the Burgers vector $a/2[01\bar{1}]$ in the projection plane are $a/4[\bar{1}1\bar{2}]$ and $a/4[110]$, respectively, and the \mathbf{b}_e and the \mathbf{b}_s related to the Burgers vector $a/2[\bar{1}0\bar{1}]$ are $a/4[\bar{1}1\bar{2}]$ and $a/4[\bar{1}\bar{1}0]$, respectively. The component of the \mathbf{b}_e is inclined at 54.44° to the interface, and only one extra half plane exists. In the projection plane of the atomic arrangement of the 90° dislocation, two extra half planes exist,

and the Burgers vector is parallel to the interface, as shown in Fig. 6. This Burgers vector lying in the (001) plane is $a/2[\bar{1}10]$. The two extra half planes of the atomic arrangement of the 90° dislocations are $(1\bar{1}1)$ and $(\bar{1}11)$, and they have a symmetric arrangement around the core in a 90° dislocation.

In summary, AES and SIMS measurements showed that the ZnTe/GaAs heterostructures had relatively sharp heterointerfaces. TEM and selected-area electron-diffraction measurements showed that 60° and 90° dislocations existed in the ZnTe/GaAs heterointerfaces. Possible atomic arrangements of the 60° and the 90° dislocations near the ZnTe/GaAs heterointerface were proposed.

The work at Kwangwoon University was supported in 2000 by the Korea Science and Engineering Foundation through the Quantum Science Research Center at Dongguk University, and the work at the Korea Advanced Institute of Science and Technology was supported by the Ministry of Science and Technology through the National Research Laboratory program.

- ¹R. F. C. Farrow, G. R. Jones, G. H. Williams, and I. M. Young, Appl. Phys. Lett. **39**, 954 (1981).
- ²J. Qiu, J. M. Depuydt, H. Cheng, and M. A. Haase, Appl. Phys. Lett. **59**, 2992 (1991).
- ³Z. Yu, S. L. Buczkowski, M. C. Petcu, N. C. Giles, and T. H. Myers, Appl. Phys. Lett. **68**, 529 (1996).
- ⁴A. Iribarren, R. Castro-Rodriguez, F. Callero-Briones, and J. L. Pena, Appl. Phys. Lett. **74**, 2957 (1999).
- ⁵H. Nakata, K. Yamada, and T. Ohyama, Appl. Phys. Lett. **74**, 3480 (1999).
- ⁶C. Jordan, J. F. Donegan, J. Hegarty, B. J. Roycroft, S. Taniguchi, T. Hino, E. Kato, N. Noguchi, and A. Ishibashi, Appl. Phys. Lett. **74**, 3359 (1999).
- ⁷K. J. Mackey, P. M. G. Allen, W. G. Herreden-Harker, and R. H. Williams, Appl. Phys. Lett. **49**, 354 (1986).
- ⁸T. W. Kim, Y. H. Chang, Y. D. Zheng, A. A. Reeder, B. C. McCombe, R. F. C. Farrow, T. Temofonte, F. A. Shirland, and A. Noreika, J. Vac. Sci. Technol. B **5**, 980 (1987).
- ⁹T. W. Kim, H. L. Park, J. Y. Lee, and H. J. Lee, Appl. Phys. Lett. **65**, 2597 (1994).
- ¹⁰N. V. Sochinskii, V. Munoz, V. Bellani, L. Vina, E. Dieguez, E. Alves, M. F. da Silva, J. C. Soares, and S. Bernardi, Appl. Phys. Lett. **70**, 1314 (1997).
- ¹¹Y. Rajakarunayake, B. H. Cole, J. O. McCaldin, D. H. Chow, J. R. Soderstorm, T. C. McGill, and C. M. Jones, Appl. Phys. Lett. **55**, 1217 (1989).
- ¹²Y. W. Mo, B. S. Swartzentruber, R. Kariotis, M. B. Webb, and M. G. Lagally, Phys. Rev. Lett. **63**, 2393 (1989).
- ¹³M. Ekawa and T. Taguchi, Jpn. J. Appl. Phys., Part 2 **28**, L1341 (1989).
- ¹⁴Y. Hishida, T. Tada, and T. Yamaguchi, J. Cryst. Growth **117**, 396 (1992).
- ¹⁵B. Quhen, W. S. Kuhn, A. Lussou, and O. Gorochoy, J. Cryst. Growth **159**, 138 (1996).
- ¹⁶W. Xuehua, A. A. Tikhonova, D. E. Sklovski, N. A. Kiselev, and W. Zigin, Philos. Mag. A **70**, 277 (1994).
- ¹⁷N. Otsuka, C. Choi, L. A. Kolodziejki, R. L. Gunshor, R. Fisher, C. K. Peng, H. Morkoc, Y. Nakamura, and S. Nagakura, J. Vac. Sci. Technol. B **4**, 896 (1986).
- ¹⁸J. W. Matthews, J. Vac. Sci. Technol. **12**, 126 (1975).
- ¹⁹A. F. Schwartzman and R. Sinclair, J. Electron. Mater. **20**, 805 (1991).
- ²⁰S. Bauer, A. Rosenauer, J. Skorsetz, W. Kuhn, H. P. Wagner, J. Zweck, and W. Gebhardt, J. Cryst. Growth **117**, 297 (1992).
- ²¹J. Hornstra, J. Phys. Chem. **5**, 129 (1958).
- ²²J. P. Hirth and J. Lothe, *Theory of Dislocations*, 2nd ed. (Wiley, New York, 1982).
- ²³B. D. Gerthsen, F. A. Ponce, and G. B. Anderson, Philos. Mag. A **59**, 1045 (1989).